Environmental Science & Technology

Article

pubs.acs.org/est

Global Transport and Deposition of ^{137}Cs Following the Fukushima Nuclear Power Plant Accident in Japan: Emphasis on Europe and Asia Using High−Resolution Model Versions and Radiological Impact Assessment of the Human Population and the Environment Using Interactive Tools

Nikolaos Evangeliou,*[,†] Yves Balkanski,[†] Anne Cozic,[†] and Anders Pape Møller[‡]

[†]Laboratoire des Sciences du Climat et de l'Environnement (LSCE), CEA-UVSQ-CNRS UMR 8212, Institut Pierre et Simon Laplace, L'Orme des Merisiers, F-91191 Gif sur Yvette Cedex, France

[‡]Laboratoire d'Ecologie, Systématique et Evolution, CNRS UMR 8079, Université Paris-Sud, Bâtiment 362, F-91405 Orsay Cedex, France.

Supporting Information

ABSTRACT: The earthquake and the subsequent tsunami that occurred offshore of Japan resulted in an important loss of life and a serious accident at the nuclear facility of Fukushima. The "hot spots" of the release are evaluated here applying the model LMDZORINCA for ^{137}Cs. Moreover, an assessment is attempted for the population and the environment using the dosimetric scheme of the WHO and the interactive tool ERICA, respectively. Cesium-137 was deposited mostly in Pacific and Atlantic Oceans and North Pole (80%), whereas the rest in the continental areas of North America and Eurasia contributed slightly to the natural background (0.5−5.0 kBq m^{-2}). The effective dose from ^{137}Cs and ^{134}Cs (radiocesium) irradiation during the first 3 months was estimated between 1−5 mSv in Fukushima and the neighboring prefectures. In the rest of Japan, the respective doses were found to be less than 0.5 mSv, whereas in the rest of the world it was less than 0.1 mSv. Such doses are equivalent with the obtained dose from a simple X-ray; for the highly contaminated regions, they are close to the dose limit for exposure due to radon inhalation (10 mSv). The calculated dose rates from radiocesium exposure on reference organisms ranged from 0.03 to 0.18 μGy h^{-1}, which are 2 orders of magnitude below the screening dose limit (10 μGy h^{-1}) that could result in obvious effects on the population. However, these results may underestimate the real situation, since stable soil density was used in the calculations, a zero radiocesium background was assumed, and dose only from two radionuclides was estimated, while more that 40 radionuclides have been deposited in the vicinity of the facility. When monitoring data applied, much higher dose rates were estimated certifying ecological risk for small mammals and reptiles in terms of cytogenetic damage and reproduction.

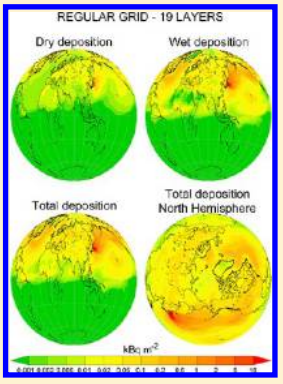

INTRODUCTION

On March 11, 2011 (14:46 local time), a great earthquake occurred in Eastern Japan (Tohoku District) resulting in severe damage to the area and to the residents. The magnitude was estimated to be 9.0 causing a large number of deaths. Due to the earthquake, big tsunamis developed and hit the Eastern Coast of Japan.[1] There are 17 nuclear power plants (NPPs) in 13 prefectures of Japan consisting of 54 reactors. In Fukushima prefecture, 10 boiling water reactors (BWR) were operated. The Fukushima Dai-ichi NPP located on the East Coast (Supporting Information Figure S2) was also attacked by the tsunamis and a simultaneous loss-of-offsite power took place. The offsite power lines were lost due to damage of the breakers and 12 emergency diesel generators (EDGs) automatically started.[2] The four BWRs were hit by the first tsunami 41 min after the earthquake and by the second one 8 min later. The ground level of the site is 10 m above sea level, and the tsunami reached 4−5 m above ground level.[3] When the tsunamis entered the NPP, the emergency generators of the stations lost their capabilities, and electric power was disrupted.[4,5] As a result, the cooling systems were damaged, internal pressure levels increased due to extreme heating of the cooling water, and hydrogen explosions occurred during March 12−15. A lot of fission products including ^{131}I, ^{134}Cs, and ^{137}Cs were released into the environment. The refractory radioactive materials (e.g., Pu isotopes) were deposited close to the NPP, whereas the most labile ones (e.g., cesium and iodine isotopes) were transported as a fallout plume over long distances following the prevailing meteorology. The rainfall started in Japan on March 15, so the radioactive materials were deposited due to wind direction and rainfall northwesterly from the NPP.

The objective of the present paper is to study the global transport and deposition of the ^{137}Cs released after the

Received: January 27, 2013
Revised: April 24, 2013
Accepted: May 1, 2013
Published: May 1, 2013

Fukushima NPP accident. An additional motive is to evaluate the efficiency of the model for ^{137}Cs using real-time measurements of surface activity concentrations obtained by the Comprehensive Nuclear-Test-Ban Treaty Organization (CTBTO). The activity concentrations of ^{137}Cs used for the comparison are available from the work of Christoudias and Lelieveld.[6] Four different simulations were carried out (i) using a regular grid (2.5° × 1.27°) over 19 vertical levels, (ii) using the same horizontal resolution over 39 vertical layers, and a combined experiment with emphasis in (iii) Europe and (iv) Asia. The aforementioned experiments in Europe and Asia were performed with simulations over a "stretched" grid, the first one pointing to Europe and the second to Asia achieving a maximum resolution of 0.45° × 0.51° over 19 vertical layers. The results were combined with those from the regular grid run, in order to map the global deposition of ^{137}Cs emphasizing over Europe and Asia. The importance of using modeling tools to predict the transport and deposition of radioactive tracers is of extreme urgency nowadays taking into account the large global risk of human exposure to radiation. Butler[7] reported an interactive map of the population residing near NPPs recording a large risk over Southeastern Asia and Europe and across the East Coast of the United States. He estimated that a major reactor accident could expose around 30 million people to radioactivity[8] in West Europe and South Asia; though a reliable model would be an asset. Finally, a risk assessment is attempted, both for the population, as well as for the environment using the dosimetric scheme of the World Health Organization (WHO)[9] and software recommended by the IAEA (the ERICA Tool[10]—see also the Supporting Information).

EMISSION OF ^{137}CS AFTER THE ACCIDENT

During nuclear accidents, radionuclides are released into the atmosphere and transported over long distances. Cesium-137 (30.2 years) is of major concern, due to its high volatility, the radiation type it emits and its biological activity (chemical analogue of potassium). Therefore, transport and removal of ^{137}Cs from the atmosphere is of major importance, as seen after the Chernobyl accident.[11−17] It has been found attached mainly to ambient (0.1−1 μm diameter) aerosol, specifically to the inorganic one,[18] and thus it is highly subject to washout removal from the contaminated air masses.[19]

As regards emissions from Fukushima, ^{137}Cs was attached in the size range 0.1−2 μm diameter.[20] These aerosols grow by coagulation during transport,[18] and are removed from the atmosphere by wet and dry deposition. Cesium-137 was still measurable before the accident at trace levels (<1 μBq m^{-3} in Central Europe[21,22] and <0.3 μBq m^{-3} in Northern and Southern Europe[23]). Its persistence in the atmosphere can be explained in terms of its long half-life (effective and physical) and inputs through resuspension from former deposition (Chernobyl or nuclear weapon testing) or through the emission of flying ashes during biomass burning.[24]

In the atmosphere, there were multiple release events in the first weeks that delivered the bulk of the radioisotopes to regions downwind (several weeks of venting, explosions, and fires at the facility). Nevertheless, the scientific community still argues about the exact amounts of the release addressing the lack of good source emission information, including locations and altitude, time variations of release rates, and physicochemical compositions. Uncertainties in model-predicted concentrations and depositions are directly related to uncertainties in source emission release rates.

Chino et al.[25] and recently Terada et al.[26] reported the total release for ^{137}Cs to be approximately 13 PBq, based on an inverse estimation of the source-term.[27] They estimated emissions using data from Japanese stations only and a regional simulation domain and, also, assuming constant radioactivity ratios for the different radionuclides based on iodine and cesium concentrations in rain, snow, and vegetation; though they mentioned large emission uncertainties (at least a factor of 5). Moreover, Povinec[28] and Kim et al.[29] reported the same total emission based upon the first estimates, whereas the French Institute of Radioprotection and Nuclear Safety (IRSN) reported releases of ^{137}Cs to be 20.6 PBq.[30] In the present study, we adopted the emission inventories for ^{137}Cs for March and April 2011, reported by Stohl et al.[31] estimated by inverse modeling (36.7 PBq). These estimates have been backed up by comparisons with measurements[6] showing relatively good correlations (^{133}Xe, ^{137}Cs, and ^{131}I).

METHODOLOGY

Model Description, Basic Scheme, and Simulations. The coupled model LMDZORINCA was used in the simulations for the accident,[3233] (see also the Supporting Information) consisting of the aerosol module INCA (INteractions between Chemistry and Aerosols), the general circulation model, LMDz (Laboratoire de Météorologie Dynamique), and the global vegetation model ORCHIDEE (ORganizing Carbon and Hydrology In Dynamic Ecosystems Environment). The model accounts for emission, transport, photochemical transformations, and scavenging (dry and wet) of chemical species and aerosols interactively in the GCM. The model can be run in a nudged mode, relaxing to ECMWF (European Centre for Medium-Range Weather Forecasts) meteorology.[34]

The simulations for the Fukushima accident were performed using the regular grid achieving maximum horizontal resolution of 2.5° in longitude and 1.27° in latitude. On the vertical two different resolutions were used for the regular grid: 19 levels extending from the surface up to about 3.8 hPa and 39 vertical layers extending from the surface up to the mesopause. However, the GCM also offers the possibility to stretch the grid over specific regions using the same number of grid-boxes. In the present study the zoom version was used for Europe and Asia achieving a horizontal resolution of 0.45° × 0.51° for 19 vertical levels. The motivation of these high resolution simulations was to construct a detailed global deposition map for ^{137}Cs combining these runs with the regular grid run. Moreover, all the dose calculations for Japan have been performed using this version obtaining a much better resolution. The final result is a global map of 2.5° × 1.27° resolution consisting of two detailed windows of 0.45° × 0.51° resolution for Europe and Asia. Each simulation lasted from March to December 2011. According to relevant measurements of ^{137}Cs activity concentrations, the detection of ^{137}Cs in the ambient aerosol ended on April 2011;[35−38] therefore, this period is considered to be sufficient in order to obtain an overall view of the global deposition of ^{137}Cs.

Dosimetric Calculations for Humans and for the Environment. Dosimetric quantities are needed to assess human radiation exposures in a quantitative way. The International Commission on Radiological Protection (ICRP) provides a system of protection against the risks from exposure

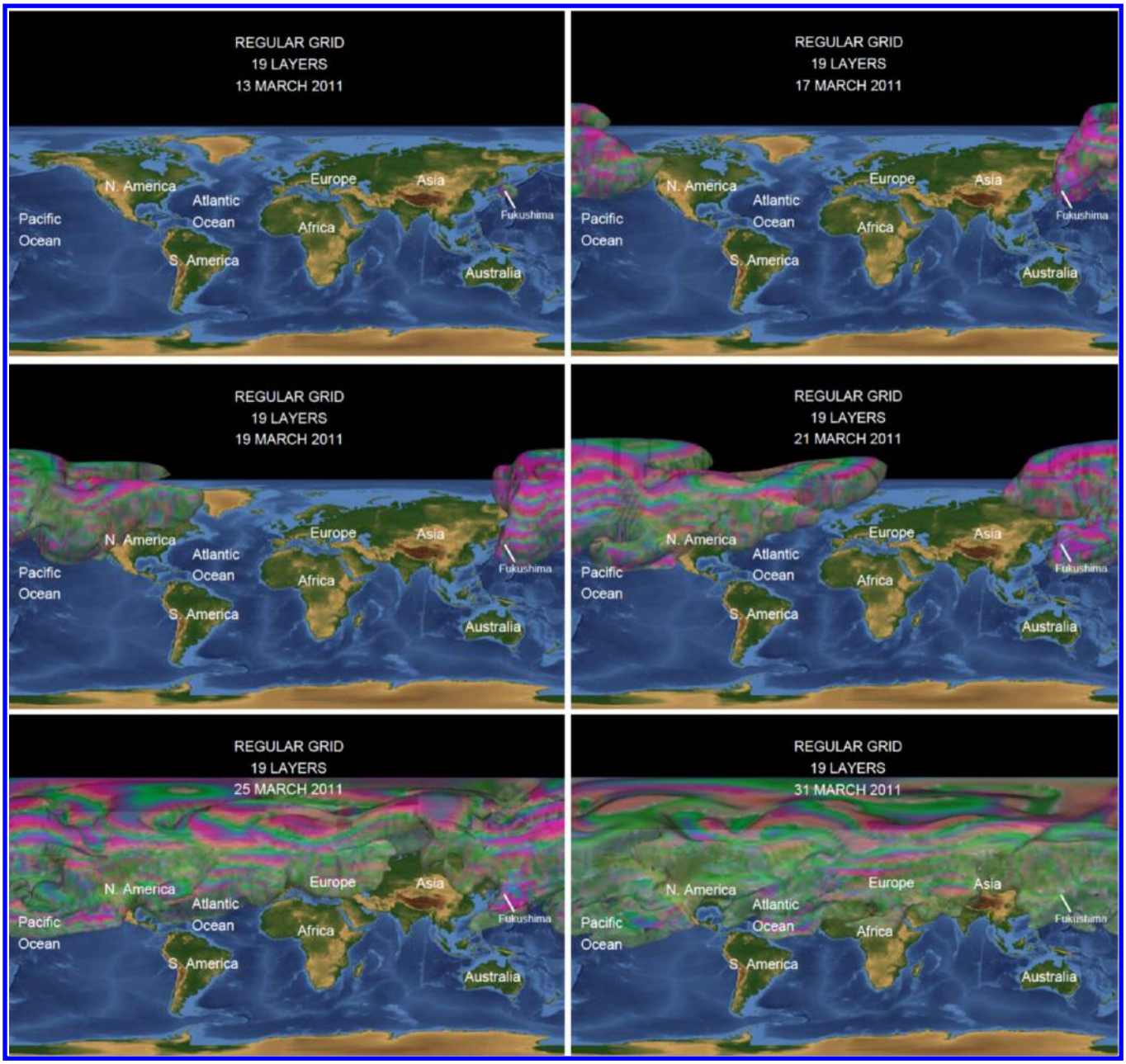

Figure 1. First arrival date of Fukushima radioactive substances at various sites in the Northern Hemisphere (West and East Coast of the USA, Europe, and Asia) as a three-dimensional representation of ^{137}Cs iso-surface (0.8 mBq m^{-3} STP). Red denotes the maximum activity, whereas blue shows the minimum one (range of the iso-surface 0−1.6 mBq m^{-3} STP).

to ionizing radiation, including recommended dosimetric quantities.[39] The dosimetric scheme for the calculations of human dose rates was adopted from WHO.[9] External doses from radionuclide deposition represent a significant long-term exposure pathway; hence it was integrated over the first year for locations both in Japan and in the rest of the world. In the study, the external effective dose from ^{137}Cs and ^{134}Cs (from now on mentioned as radiocesium) deposited on the ground was calculated. Cesium-134 ($t_{1/2}$ = 2.065 y) concentrations and deposition rates in each grid cell and time step were calculated from ^{137}Cs assuming a ^{134}Cs/^{137}Cs isotopic ratio of 0.92, based on CTBTO observations following the accident.[6,40] Moreover, the external effective dose from the presence of radiocesium in the radioactive cloud (fallout), the effective dose from inhalation and the dose from ingestion of radioactive materials were also estimated using the same scheme.

Dosimetric Modeling of the Ecosystem Using the ERICA Tool. Since the Chernobyl accident, a great challenge in radioecology has been the development of a tool that will be able to record and assess the changes in the population of nonhuman biota due to effects from ionizing radiation. For this reason, a supporting computer-based tool (the ERICA tool) has been developed (see also the Supporting Information),[41,42] which guides the user through the assessment process, recording information and decisions, and allowing the necessary calculations to estimate risks to selected animals and plants.[10,43] The results can be put into context using incorporated databases on dose effects, relationships, and background dose rates. In the present assessments the Tier 2

dx.doi.org/10.1021/es400372u | Environ. Sci. Technol. 2013, 47, 5803−5812

scheme was used for dose rate calculations from radiocesium to the terrestrial reference organisms, namely amphibians, birds, bird's eggs, detritivorous invertebrates, flying insects, gastropods, grasses and herbs, lichens and bryophytes, mammals (rat), reptiles, shrub, soil invertebrates (worms), and trees.

RESULTS AND DISCUSSION

Global Fallout Transport from Fukushima NPP and Comparison with Measurements. In the first days after the power loss, Tokyo Electric Power Company (TEPCO), the operator of the NPP, vented the reactors to relieve the pressure in the containment and to prevent explosions. During the initial period the winds were predominantly from the northwest (prevailing direction in mid-March), directed offshore and therefore transporting the plume over the ocean. For several hours on March 15 the winds were onshore (from the Southeast). Source term estimates published rapidly by the Japan Atomic Energy Agency (JAEA),[25] as well as other modelers,[31] established that the greatest release occurred in March 15, when explosions rocked several of the reactors and fires were ongoing at the spent fuel pool. This event spread radioisotopes along a band through the mountains and affected areas more than 30 km from the plant. Then on March 21 the winds blew toward the south and southeast toward the outer regions of Tokyo (Supporting Information Figure S1; also reported by Kinoshita et al.[44]). The two vertical resolutions used for this simulation (19 and 39 levels) did not show any significant differences in the transport of ^{137}Cs on the vertical. The reason is that the releasing heights[31] introduced ^{137}Cs within three atmospheric layers (50, 300, and 1000 m) layered with large distances in between. Obviously, the distribution of ^{137}Cs in the vertical levels did not affect its transport.

As regards to the global transport of ^{137}Cs from Fukushima (Figure 1), the fallout was dispersed from Eastern Asia to Europe and back to Asia presenting very similar ^{137}Cs activity concentrations (Figure 1). The ^{137}Cs activity concentrations in Figure 1 are expressed in becquerels per cubic meter STP, where cubic meter STP is a standard cubic meter of air at 273.15 K temperature and 1 atm pressure. During the first 36 h of simulation, the majority of radioactive emissions were advected eastward over the Pacific Ocean. A week into the simulation, radioactivity had spread throughout the Northern Pacific, reaching the contiguous United States, Alaska, and Russia (Figure 1). The radioactive plume arrived on the West Coast of the US on March 16–17, 2011, whereas Bowyer et al.[45] and Diaz Leon et al.[46] reported that airborne fission products, including ^{131,132}I, ^{134,137}Cs, ^{132}Te, and ^{133}Xe were first detected on the West Coast of the US on March 16th. In addition, the US EPA[47] reported that the Fukushima plume of radiocesium arrived in California on March 18th. By the second week of the simulation, radioactivity had spread across the Atlantic but had not crossed the Equator (Figure 1). Cesium-137 fallout reached the Northeast Coast of the USA on March 19th, 2011, and Orlando on March 21st, 2011, although Hernández-Ceballos et al.[48] reported that it was initially detected in Orlando (Southeastern USA) on March 24th, 2011. This deviation might be attributed to the nature of the sampling techniques used for aerosol identification presenting large filtrating instruments at the surface, where air is passed through selective filters, achieving a limit of detection on the order of microbecquerels per cubic meter; in contrast, modeling results give concentrations several orders of magnitude lower. The plume then moved toward the North Atlantic approaching Iceland and Norway on March 20th (arrival on March 21st reported by Masson et al.[35]) and up to South Korea by the end of March (arrival on April 1–3 reported by Hernández-Ceballos et al.[48]). By the third week of the simulation, radioactivity was relatively well-mixed throughout the Northern Hemisphere (Figure 1). Dust deposited at Uljin (South Korea) was contaminated with ^{137}Cs derived from Fukushima reaching values larger than 200 Bq kg^{-1},[48] although the respective concentrations prior to the accident were about 50 Bq kg^{-1}. These observations in conjunction with the global fallout evolution presented by our model prove that the surrounding South Korea was disconnected from the Northeast Coast of Japan in March and attacked by the attenuated fallout after full-globe transport. However, the model results (Figure 1) display that in late March there was a small direct transport of ^{137}Cs to the South Korean region, which is also certified by low measurements of radiocesium in Chuncheon and in Uljin.[48] Hong et al.[49] reported that these lower concentrations were derived by the progressive downward movement of radionuclides released from Fukushima and then accumulated at higher latitudes.

The results from the comparison of the modeled ^{137}Cs activity concentrations with the CTBTO measurements taken from the work of Christoudias and Lelieveld[6] can be found in Figures S3a–c in the Supporting Information. The model results presented here are daily averages of ^{137}Cs activity concentrations in the lowest layer of the model and in the grid-boxes where the stations are located. It is noteworthy that there is good agreement of the arrival times of ^{137}Cs plume at each station, the first detection time and the major concentration peaks, especially for stations in North America, North Europe, and the West Pacific, taking into account the source uncertainties. An additional uncertainty in the arrival times might be attributed to the fact that CTBTO stations collect samples every 12 h or more; therefore uncertainties of 1 day can be assumed for each measurement station. In many cases records are not continuous and no observations for the arrival of ^{137}Cs plumes were available. Despite all the limitations, there is good coherence between model and measured concentrations. A better coherence was obtained using the larger vertical resolution (39 levels) on a global scale.

Deposition of ^{137}Cs with Emphasis on Europe and Asia. During the first week after the accident (March 11–15), when deposition rates increased over the areas around Fukushima, northeasterly or easterly winds associated with a transient cyclone transported and deposited ^{137}Cs from the NPP to inland areas (Figure 2). On the other hand, precipitation was observed during the second week after the accident (March 15–22); a cyclone passed over Japan, and ^{137}Cs was effectively deposited over land. During the same period (March 17–20), when an anticyclone prevailed over Fukushima, ^{137}Cs was transported and deposited to the Pacific Ocean and the West Coast of the USA (Figure 2). Although the emissions from Fukushima continued in the 3 weeks after the accident, they were 3–4 orders of magnitude lower; therefore, a decreased contribution was observed in the deposition inventory of Japan (1–10 kBq m^{-2}) and the North Pacific (up to 10 kBq m^{-2}), whereas traces were deposited in the USA (<0.5 kBq m^{-2}), in the Atlantic Ocean (<1 kBq m^{-2}), in Europe (maximum 0.1 kBq m^{-2}), and in Asia (<0.05 kBq m^{-2}). Finally, precipitation was extremely low in the Northern Hemisphere during the first week of April (week 4), thus no intense deposition was observed (Figure 2), despite

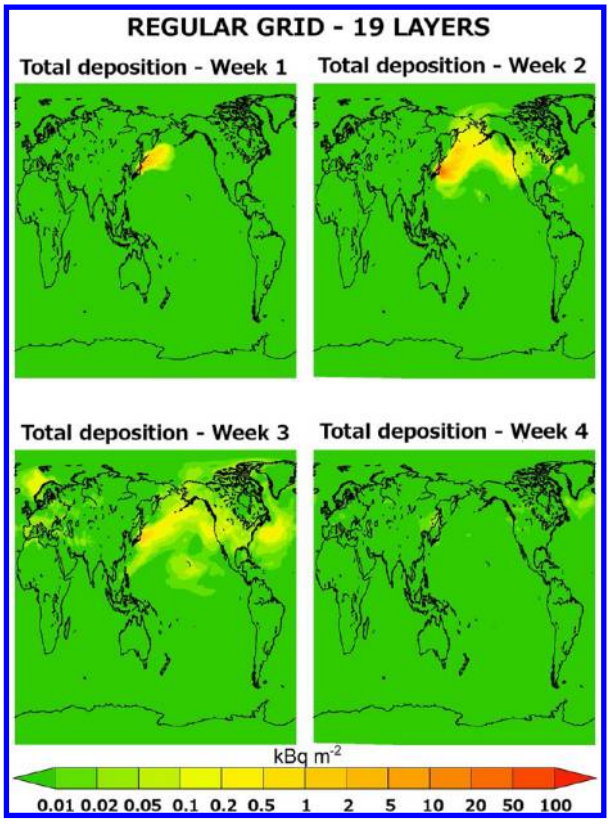

Figure 2. Total deposition of ^{137}Cs (kBq m^{-2}) during the first 4 months after the accident. The deposition is expressed in weekly intervals.

the large emissions from the NPP (in the order of 10^{13} Bq per day). These trends are in good agreement with previously published results[40,50] and, also, with the overall amount of ^{137}Cs deposited in inland areas, estimated to be 20%, while the rest was deposited in the World Ocean, as well as in the North Pole glaciers.[6,50]

The global deposition of ^{137}Cs is shown in Figure 3 in terms of cumulative values for 2011. For this figure the results of three simulations were used: a run in the regular grid (2.5° × 1.27°), another with the grid stretched over Europe, and another run over Asia (0.45° × 0.51°) for 19 vertical levels. Following the definitions of the International Atomic Energy Agency,[51,52] any area with deposition inventory more than 40 kBq m^{-2} is considered to be contaminated; therefore the maximum in the scale used was 40 kBq m^{-2}. However, from the combined map, it was found that the highest depositions occurred around the NPP's grid-cells, with deposition exceeding the contamination limit and affecting an area of over 9 million inhabitants.[6] The average deposition in the NPP's grid-cell was in the range of megabecquerels per square meter. Noticeably, very low deposition was observed in Europe presenting values below 0.1 kBq m^{-2}. The highest inventories were calculated for South Europe and also for Turkey. These values are radiologically insignificant having invisible impact on humans and the environment. The same situation was observed in Asia with deposition inventories far below the limit derived from IAEA guidelines (Figure 3).

Risk Assessment to the Population from the Fukushima NPP Accident. This section provides data on effective doses of the public resulted from exposure within the first year after the accident worldwide, with greater detail inside Japan. The assessment was performed to provide dose estimates and is based on information publicly available by the Japanese authorities. The results of the dose estimates are validated with reports from the WHO and with comparisons

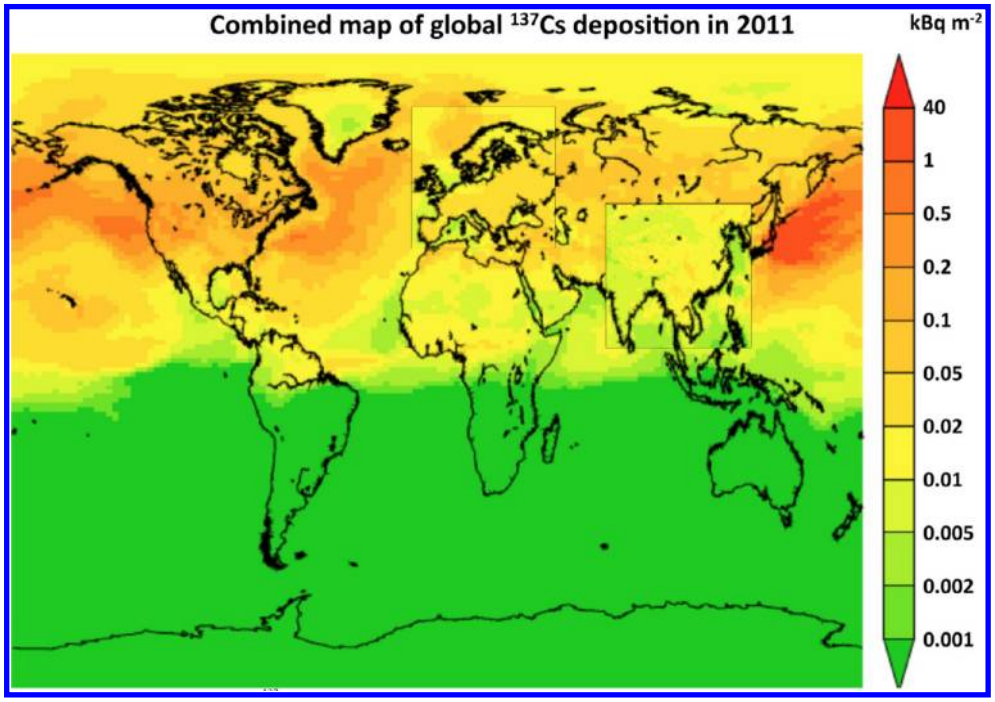

Figure 3. Total cumulative deposition of ^{137}Cs in 2011. Results of three different simulations were used: a run in the regular grid (2.5° × 1.27°), another with the grid stretched over Europe achieving a maximum resolution of 0.45° × 0.51°, and another run using a stretched grid over Asia (0.45° × 0.51°).

dx.doi.org/10.1021/es400372u | Environ. Sci. Technol. 2013, 47, 5803−5812

with data on human in vivo monitoring measurements (e.g., whole body counting).

The input data were modeling results of ^{137}Cs and calculated results of ^{134}Cs (from the respective isotopic ratio) in the environment (soil and aerosol concentrations) and parameters taken from WHO[9] in foodstuffs. The methodology used to calculate the doses relies on the most recent dosimetric and biokinetic models for different population subgroups (i.e., infants, children, and adults), although here only dose rates to adults are presented. The dosimetric scheme considers all major routes of exposure: (i) the external exposure from the presence of radiocesium (^{137}Cs and ^{134}Cs) in the fallout and on the ground and (ii) the internal exposure from ingestion of foodstuffs and inhalation of radiocesium.

Given the limited information available, the assessment contains a number of assumptions (e.g., fallout composition and dispersion, time spent indoors/outdoors, and consumption levels). All efforts were made to avoid any underestimation of doses. In this context, the assessment showed that the cumulative effective dose from deposition, fallout presence (external), and inhalation received by adults until the end of 2011 in areas outside of Japan was below 0.05 mSv and usually far below this level (Figure 4), which agrees well with the

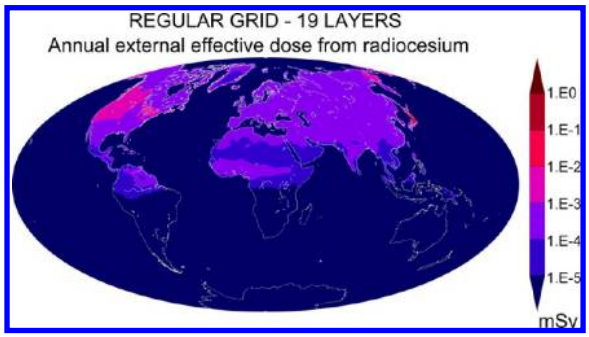

Figure 4. Global map of effective doses from radiocesium (^{137}Cs and ^{137}Cs) as a result of exposure during the first three months after the Fukushima Dai-ichi accident. The external exposure due to the presence of radiocesium in the radioactive fallout (air-submersion), the external irradiation from radiocesium deposition, and the internal inhalation pathway has been taken into consideration. Food-ingestion assumed to be negligible for the global population as monitoring has been activated after the accident preventing contaminating food to be imported by the countries according to the national regulations.

records of WHO. Maxima were calculated for the West Coast of the USA (1−10 μSv), whereas estimates in Eurasia were found to be below 0.1 μSv. It has previously been suggested that during the first months fallout remained confined to the Northern Hemisphere, with the Equator acting as a dividing line. Although traces of radiocesium have been reported in the Southern Hemisphere, the external effective doses from radiocesium were one-fifth and probably less than those in the Northern.

As regards to the effective dose over Japan, both external and internal doses for the three first months (March−May) were taken into consideration (Figure 5). The experience of Chernobyl showed that the effective dose rates decrease within the first year after the accident mainly due to radioactive decay of the short-lived radionuclides. However, a term that minimizes the dose in that case is that atmospheric burden can be neglected after the first year of the accident; thus, inhalation dose and the dose from air-submersion of radio-

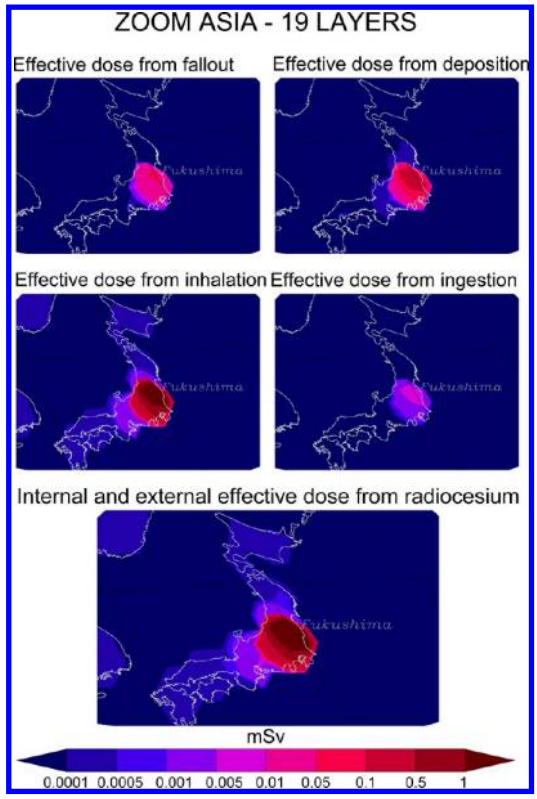

Figure 5. External (from radiocesium presence in fallout and ground deposition) and internal (inhalation and ingestion) cumulated effective doses during the first three months after the accident. The foodstuffs account for the ingestion of radiocesium are cereals, green vegetables, root vegetables, orchard fruits, soft fruits, milk, beef, lamp, fish, and mushrooms.

cesium tend to zero. In addition, the dose from radiocesium deposition has been found to decrease during the following decade due to radioactive decay of ^{134}Cs and the vertical migration into the soil.[53,54] The shielding effect of soil migration is an important factor in reducing doses. About 30% of the effective dose has been estimated to decrease during the first year, while about 70% during the first 15 years.[55] More specifically, the total cumulative effective dose (deposition, fallout, inhalation, and ingestion) in Fukushima prefecture (Northwest of the Fukushima NPP) during the first three months is within a dose band of 1−5 mSv. In these most affected regions, inhalation dose is more significant during the first month after the accident decreasing in the next two months (Supporting Information Figure S6). Cumulative effective doses of radiocesium in the rest of Japan were estimated to be within 0.001−0.5 mSv.

The estimation of doses from food is another important factor in the assessment of overall doses. For Fukushima prefecture the estimated effective dose from food ingestion per month was highest in March 2011 and decreased until August (Supporting Information Figure S4). The estimated effective dose to adults in the Fukushima prefecture from one year's intake of radionuclides in food was estimated as 0.2 mSv, whereas the dietary exposure outside Fukushima is two times lower. It should be stated that the dietary exposure assessment is for Japanese consumers only consuming exclusively food produced in areas where food monitoring was implemented. However, measurements in eggs, rice, and tap water were not available in order to include them in the dose estimations,

although doses from tap water have been reported to be low (e.g., 9 μSv per month reported by Hamada and Ogino[56] in tap water) compared to the doses from other intake pathways (Supporting Information Figure S4). Harada et al.[57] reported that the annual mean dose rate from radiocesium ingestion was 0.026 ± 0.020 mSv in the Fukushima prefecture showing that the model calculated ingestion dose rates might be overestimated.

In order to assess the importance and impact of the estimated doses to humans from many areas of the world, they are compared with exposures arising from other sources. The United Nations Scientific Committee on the Effects of Atomic Radiation (UNSCEAR) has estimated that the global average effective dose per person from all natural and artificial sources of radiation in the environment is approximately 3.0 mSv per year.[58] About 80% of the annual radiation dose that a person receives is due to natural radiation from cosmic rays, the earth, and naturally occurring radionuclides in food and drink. People receive an average of 2.4 mSv[58] per year through this natural exposure. Due to geological differences, people may receive annual effective doses significantly higher than the global average. The most significant manmade sources of human exposure are radiological medical investigations and treatment.[59] According to the dose calculation for the first year after the accident, the dose levels from radiocesium can be compared with those of a simple medical exposure (e.g., dental X-ray 0.005 mSv or chest X-ray 0.02 mSv) for the areas outside Japan. For the Fukushima territory, the effective doses are similar to those of X-ray computed tomography scan (2 mSv) or abdomen, pelvis, or lumbar X-ray (0.7−1 mSv) contributing up to 30% on the average effective dose from all natural and artificial sources (3 mSv per year). In the rest of Japan the obtained doses can be compared with those due to exposure to cosmic rays during transoceanic flights (e.g., Seoul−Montreal 0.1 mSv, New York−Tokyo 0.07 mSv). Finally, whole body measurements performed to inhabitants of the "restricted area" and the "deliberate evacuation area" [9] showed that the internal effective doses from radiocesium were less than 2 mSv in total, and in the vast majority (99.8%) were less than 1 mSv, assuming that the intake of radioactivity into the body occurred by inhalation on March 12, 2011, whereas the respective inhalation doses for the same date were 0.63 μSv (<1 mSv).

These estimates are from a theoretical point of view and do not pose the overall situation especially in the contaminated areas. After a nuclear accident (e.g., Chernobyl) the heavy debris, consisting of transuranium elements dominates the local fallout and is deposited in the vicinity of the damaged plant.[60] Given that in Fukushima more than 45 different radionuclides have been released of the order of GBq,[30] one should expect enhanced doses comparing to those estimated here. However, the radiation protection actions made from the very early days after the accident (evacuation and provision of stable iodine tablets) prevented greater radiological damage to the population.

Environmental Risk Assessment from Ionizing Radiation in Japan. The ERICA tool was processed for the reference organisms of the terrestrial ecosystem. Average dose rates (μGy h^{-1}) for 5-day intervals were calculated providing the 5-day average surface activity concentration of the most contaminated area in Japan. In addition, the surface soil activity concentrations were also calculated (5-day averages) assuming no background radioactivity of radiocesium and a stable soil density (1.6 gr cm^{-3}) and doses were calculated. The resulting dose rate patterns, expressed as internal and external dose rate averages, are shown in Supporting Information Figure S5 for the highest contamination area (NPP's grid-box). The dose rates for the selected reference organisms ranged from 0.03 to 0.18 μGy h^{-1} (total exposure), which are far below the screening dose limit (10 μGy h^{-1}) that could harm the abundance of a population. In order to be able to compare the observed effects of radiation on reference organisms, an example is mentioned for the organism "bird" as recorded in the tool. For small grouse, irradiation with up to 10 μGy h^{-1} would result in statistically insignificant effects on the weight of birds, whereas for large grouse would lead to increases in infestations with parasites of feather sand gastroenterine. Irradiation of tree swallows with more than 30 μGy h^{-1} would result in statistically insignificant effects on breeding success measured as clutch size, hatching success, fledging number, incubation time, and nestling time. Dose rates range between 5000−10 000 μGy h^{-1} for chickens would lead to reduction in the number of oocytes contained within two-week-old birds.

No variety of measurements for doses in nonhuman biota have been recorded and published yet, that allow comparison with the obtained results in this modeling study. However, the low level chronic irradiation could lead to unpredictable effects. Møller et al.[61] reported that the relationship between radiation and abundance of common birds showed a more negative value at Fukushima than at Chernobyl demonstrating a negative consequence of radiation for birds after the accident and during the main breeding season of March−July 2011. This practically means that selection already eliminated individuals with accumulated mutations in Chernobyl to a greater extent than at Fukushima, the composition of radionuclides were more dangerous for birds at Fukushima than at Chernobyl, or the higher density at Fukushima than at Chernobyl increased the intensity of intraspecific competition. Moreover, Hiyama et al.[62] reported that the accident caused physiological and genetic damage to a lycaenid butterfly in May 2011 (mild abnormalities), whereas adult butterflies collected in September showed more severe abnormalities. In addition, Møller et al.[63] censused spiders, grasshoppers, dragonflies, butterflies, bumblebees, cicadas, and birds at Chernobyl and Fukushima-Daiichi. Given that the mean level of radiation was higher and less variable at Fukushima than at Chernobyl, more negative effects on the abundance of animals at Fukushima should be observed. However, only three out of seven taxa showed significant declines in abundance, which means that the effect of radiation on abundance differs at Fukushima due to radiotoxicity, while in the case of Chernobyl this effect is due to a mixture of radiotoxicity and mutation accumulation, because chronic exposure of many generations allowed accumulation of mutations. Moreover, Garnier-Laplace et al.[64] reported that the maximum dose rates from ^{131}I, ^{134}Cs, and ^{137}Cs in terrestrial organisms were found to be near the screening dose rate (10 μGy h^{-1}), where no obvious effects occur. Finally, Shozugawa et al.[65] published results of soil samples collected in April 2011 within 5 km from the NPP. The concentrations were 4.9×10^4 Bq kg^{-1} for ^{131}I, 5×10^3 Bq kg^{-1} for each of ^{134}Cs and ^{137}Cs, 5 Bq kg^{-1} for ^{110m}Ag, 100 Bq kg^{-1} for ^{132}Te, and 7 Bq kg^{-1} for each of ^{95}Zr and ^{95}Nb. Applying these values to the tool, we obtain dose rates between 10^{-1} and 10^2 μGy h^{-1} for the terrestrial organisms. The dose rates for birds, bird's eggs, mammals (rats), reptiles, shrub, and soil invertebrates exceeded the screening dose of 10 μGy h^{-1} showing the existence of a

dx.doi.org/10.1021/es400372u | Environ. Sci. Technol. 2013, 47, 5803−5812

potential ecological risk to the terrestrial ecosystem inside the exclusion zone.

■ ASSOCIATED CONTENT

Supporting Information

Figure S1 depicts a 3-dimensional representation of the iso-surface of ^{137}Cs in the Western Pacific Ocean in two vertical resolutions (blue to red represents the range of 0−1.6 mBq m^{-3} STP). Figure S2 presents a map of Japan with cities of population over 77 000 inhabitants. Okuma and Futaba were ordered immediate evacuation the morning following the accident. Figure S3 depicts the CTBTO measurement network. The blue rhombus denotes surface ^{137}Cs activity concentrations for the version of 19 levels, the green triangle for the version over 39 levels, whereas the black rectangles are CTBTO measurements. Figure S4 shows the effective dose from ingestion of various products and the respective percentage contribution to the total ingestion effective dose per month. Figure S5 depicts time series data of dose rates to reference organisms used in the ERICA tool. The data are daily average dose rates for 5-day intervals. Figure S6 presents the percentage contribution of different exposure pathways on the effective dose from radiocesium for the grid-box of the NPP. Finally, SI—Methodology describes the dosimetric scheme used for the dose rate calculation of the population. Also, an introduction on the principles of the ERICA tool is provided. This material is available free of charge via the Internet at http://pubs.acs.org..

■ AUTHOR INFORMATION

Corresponding Author

*Tel.: +33 1 6908-1278. Fax: +33 1 6908-3073. E-mail: Nikolaos.Evangeliou@lsce.ipsl.fr.

Notes

The authors declare no competing financial interest.

■ ACKNOWLEDGMENTS

The authors would like to acknowledge the funding source of the project (GIS Climat-Environnement-Société, http://www.gisclimat.fr/projet/radioclimfire). This work was granted access to the HPC resources of [CCRT/TGCC/CINES/IDRIS] under the allocation 2012-t2012012201 made by GENCI (Grand Equipement National de Calcul Intensif). We appreciate Dr. Olivier Evrard (LSCE) and Dr. Cyril Moulin (Director of the LSCE) for the comments and the useful discussion.

■ REFERENCES

(1) Akahane, K.; Yonai, S.; Fukuda, S.; Miyahara, N.; Yasuda, H.; Iwaoka, K.; Matsumoto, M.; Fukumura, A.; Akashi, M. The Fukushima Nuclear Power Plant accident and exposures in the environment. *Environmentalist* **2012**, *32*, 136−143.

(2) Hirano, M.; Yonomoto, T.; Ishigaki, M.; Watanabe, N.; Maruyama, Y.; Sibamoto, Y.; Watanabe, T.; Moriyama, K. Insights from review and analysis of the Fukushima Dai-ichi accident. *J. Nucl. Sci. Technol.* **2012**, *49*, 1−17.

(3) Nuclear and Industrial Safety Agency (NISA) and Japanese Nuclear Energy Safety Organization (JNES), The 2011 off the Pacific Coast of Tohoku Pacific Earthquake and the Seismic Damage to the NPPs. http://www.nisa.meti.go.jp/english/files/en20110406-1.html (July 20, 2011).

(4) Nuclear and Industrial Safety Agency (NISA) Press Releases−October 2011. http://www.nisa.meti.go.jp/english/press/index.html (October 10, 2011).

(5) Tokyo Electric Power Company (TEPCO) Press Release−May 2011. http://www.tepco.co.jp/en/press/corp-com/release/ (May 4, 2011).

(6) Christoudias, T.; Lelieveld, J. Modelling the global atmospheric transport and deposition of radionuclides from the Fukushima Dai-ichi nuclear accident. *Atmos. Chem. Phys. Discuss.* **2012**, *12*, 24531−24555.

(7) Butler, D. Reactors, residents and risk. *Nature* **2011**, DOI: 10.1038/472400a.

(8) Lelieveld, J.; Kunkel, D.; Lawrence, M. G. Global risk of radioactive fallout after major nuclear reactor accidents. *Atmos. Chem. Phys.* **2012**, *12*, 4245−4258.

(9) *Preliminary dose estimation from the nuclear accident after the 2011 Great East Japan earthquake and tsunami*; World Health Organisation (WHO): Gevena, Switzerland, 2012; http://whqlibdoc.who.int/publications/2012/9789241503662_eng.pdf; ISBN 978 92 4 150366 2.

(10) Brown, J.; Alfonso, B.; Avila, R.; Beresford, N. A.; Copplestone, D.; Prohl, G.; Ulanovsky, A. The ERICA Tool. *J. Environ. Radioact.* **2008**, *99*, 1371−1383.

(11) Albergel, A.; Martin, D.; Strauss, B.; Gros, J. -M. The Chernobyl accident: Modeling of dispersion over Europe of the radioactive plume and comparison with air activity measurements. *Atmos. Environ.* **1988**, *22*, 2431−2444.

(12) Hass, H.; Memmesheimer, M.; Geiss, H.; Jakobs, H. J.; Laube, M.; Ebel, A. Simulation of the Chernobyl radioactive cloud over Europe using EURAD model. *Atmos. Environ.* **1990**, *24*, 673−692.

(13) Bonelli, P.; Calori, G.; Finzi, G. A fast long-range transport model for operational use in episode simulation. Application to the Chernobyl accident. *Atmos. Environ.* **1992**, *26*, 2523−2535.

(14) Desiato, F. A long-range dispersion model evaluation study with Chernobyl data. *Atmos. Environ.* **1992**, *26*, 2805−2820.

(15) Salvadori, G.; Ratti, S. P.; Belli, G. Modelling the Chernobyl radioactive fallout (II): A multifractal approach in some European countries. *Chemosphere* **1996**, *33*, 2359−2371.

(16) Hatano, Y.; Hatano, N.; Amano, H.; Ueno, T.; Sukhoruchkin, A. K.; Kazakov, S. V. Aerosol migration near Chernobyl: long-term data and modeling. *Atmos. Environ.* **1998**, *32*, 2587−2594.

(17) Brandt, J.; Christensen, J. H.; Frohn, L. M. Modeling transport and deposition of caesium and iodine from the Chernobyl accident using the DREAM model. *Atmos. Chem. Phys.* **2002**, *2*, 397−417.

(18) Jost, D. T.; Gaggeler, H. W.; Baltensperger, U.; Zinder, B.; Haller, P. Chernobyl fallout in size-fractionated aerosol. *Nature* **1986**, *324*, 22−23.

(19) Seinfeld, J. H.; Pandis, S. N. *Atmospheric Chemistry and Physics: From Air Pollution to Climate Change*; John Wiley and Sons: New York, USA, 1998.

(20) Kaneyasu, N.; Ohashi, H.; Suzuki, F.; Okuda, T.; Ikemori, F. Sulphate aerosol as a potential transport medium of radiocesium from the Fukushima nuclear accident. *Environ. Sci. Technol.* **2012**, *46* (11), 5720−5726.

(21) Bieringer, J.; Schlosser, C.; Sartorius, H.; Schmid, S. Trace analysis of aerosol bound particulates and noble gases at the BfS in Germany. *Appl. Radiat. Isot.* **2009**, *67*, 672−677.

(22) Rulík, P.; Mala, H.; Beckova, V.; Holgye, Z.; Schlesingerova, E.; Svetlik, I.; Skrkal, J. Low level air radioactivity measurements in Prague, Czech Republic. *Appl. Radiat. Isot.* **2009**, *67*, 969−973.

(23) Masson, O.; Piga, D.; Gurriaran, R.; D'Amico, D. Impact of an exceptional Saharan dust outbreak in France: PM10 and artificial radionuclides concentrations in air and in dust deposit. *Atmos. Environ.* **2010**, *44*, 2478−2486.

(24) Bourcier, L.; Sellegri, K.; Masson, O.; Zangrando, R.; Barbante, C.; Gambaro, A.; Pichon, J. -M.; Boulon, J.; Laj, P. Experimental evidence of biomass burning as a source of atmospheric ^{137}Cs, Puy de Dome (1465 m a.s.l.), France. *Atmos. Environ.* **2010**, *44*, 2280−2286.

(25) Chino, M.; Nakayama, H.; Nagai, H.; Terada, H.; Katata, G.; Yamazawa, H. Preliminary estimation of release amounts of ^{131}I and ^{137}Cs accidentally discharged from the Fukushima Daiichi Nuclear Power Plant into the atmosphere. *J. Nucl. Sci. Technol.* **2011**, *48* (7), 1129−1134.

(26) Terada, H.; Katata, G.; Chino, M.; Nagai, H. Atmospheric discharge and dispersion of radionuclides during the Fukushima Dai-ichi Nuclear Power Plant accident. Part II: verification of the source term and analysis of regional-scale atmospheric dispersion. *J. Environ. Radioact.* **2012**, *112*, 141−154.
(27) Ministry of Education, Culture, Sports, Science and Technology (MEXT) Press release−June 2011. http://www.mext.go.jp/english (June 30, 2011).
(28) Povinec, P. P. Preface − Fukushima II. *J. Environ. Radioact.* **2012**, *114*, 1.
(29) Kim, C. -K.; Byun, J. -I.; Chae, J. -S.; Choi, H. -Y.; Choi, S. -W.; Kim, D. -J.; Kim, Y. -J.; Lee, D. -M.; Park, W. -J.; Yim, S. A.; Yun, J. -Y. Radiological impact in Korea following the Fukushima nuclear accident. *J. Environ. Radioact.* **2012**, *111*, 70−82.
(30) *Fukushima, one year later Initial analyses of the accident and its consequences*; Report IRSN/DG/2012−003; Institut de Radioprotection et de Surete Nucleaire (IRSN), 2012; http://www.irsn.fr/EN/publications/technical-publications/Documents/IRSN_Fukushima-1-year-later_2012-003.pdf.
(31) Stohl, A.; Seibert, P.; Wotawa, G.; Arnold, D.; Burkhart, J. F.; Eckhardt, S.; Tapia, C.; Vargas, A.; Yasunari, T. J. Xenon-133 and caesium-137 releases into the atmosphere from the Fukushima Dai-ichi nuclear power plant: determination of the source term, atmospheric dispersion, and deposition. *Atmos. Chem. Phys.* **2012**, *12*, 2313−2343.
(32) Szopa, S.; Balkanski, Y.; Cozic, A.; Deandreis, C.; Dufresne, J. -L.; Hauglustaine, D.; Lathiere, J.; Schulz, M.; Vuolo, R.; Yan, N.; Marchand, M.; Bekki, S.; Cugnet, D.; Idelkadi, A.; Denvil, S.; Foujols, M. -A.; Caubel, A.; Fortems-Cheiney, A. Aerosol and Ozone changes as forcing for Climate Evolution between 1850 and 2100. *Clim. Dyn.* **2012**, DOI: 10.1007/s00382-012-1408-y.
(33) Hauglustaine, D. A.; Hourdin, F.; Walters, S.; Jourdain, L.; Filiberti, M. -A.; Larmarque, J. -F.; Holland, E. A. Interactive chemistry in the Laboratoire de Météorologie Dynamique general circulation model: description and background tropospheric chemistry evaluation. *J. Geophys. Res.* **2004**, *109*, D04314 DOI: 10.1029/2003JD003957.
(34) Hourdin, F.; Issartel, J. P. Sub-surface nuclear tests monitoring through the CTBT xenon network. *Geophys. Res. Lett.* **2000**, *27*, 2245−2248.
(35) Masson, O.; Baeza, A.; Bieringer, J.; Brudecki, K.; Bucci, S.; Cappai, M.; Carvalho, F. P.; Connan, O.; Cosma, C.; Dalheimer, A.; Didier, D.; Depuydt, G.; De Geer, L. E.; De Vismes, A.; Gini, L.; Groppi, F.; Gudnason, K.; Gurriaran, R.; Hainz, D.; Halldorsson, O.; Hammond, D.; Hanley, O.; Holey, K.; Homoki, Zs.; Ioannidou, A.; Isajenko, K.; Jankovic, M.; Katzlberger, C.; Kettunen, M.; Kierepko, R.; Kontro, R.; Kwakman, P. J. M.; Lecomte, M.; Leon Vintro, L.; Leppanen, A. -P; Lind, B.; Lujaniene, G.; Mc Ginnity, P.; Mc Mahon, C.; Mala, H.; Manenti, S.; Manolopoulou, M.; Mattila, A.; Mauring, A.; Mietelski, J. W.; Møller, B.; Nielsen, S. P.; Nikolic, J.; Overwater, R. M. W.; Palsson, S. E.; Papastefanou, C.; Penev, I.; Pham, M. K.; Povinec, P. P.; Rameback, H.; Reis, M. C.; Ringer, W.; Rodriguez, A.; Rulík, P.; Saey, P. R. J.; Samsonov, V.; Schlosser, C.; Sgorbati, G.; Silobritiene, B. V.; Soderstrom, C.; Sogni, R.; Solier, L.; Sonck, M.; Steinhauser, G.; Steinkopff, T.; Steinmann, P.; Stoulos, S.; Sykora, I.; Todorovic, D.; Tooloutalaie, N.; Tositti, L.; Tschiersch, J.; Ugron, A.; Vagena, E.; Vargas, A.; Wershofen, H.; Zhukova, O. Tracking of airborne radionuclides from the damaged Fukushima Dai-Ichi nuclear reactors by European networks. *Environ. Sci. Technol.* **2011**, *45*, 7670−7677.
(36) Long, N. Q.; Truong, Y.; Hien, P. D.; Binh, N. T.; Sieu, L. N.; Giap, T. V.; Phan, N. T. Atmospheric radionuclides from the Fukushima Dai-ichi nuclear reactor accident observed in Vietnam. *J. Environ. Radioact.* **2012**, *111*, 53−58.
(37) McMullin, S.; Giovanetti, G. K.; Green, M. P.; Henning, R.; Holmes, R.; Vorren, K.; Wilkerson, J. F. Measurement of airborne fission products in Chapel Hill, NC, USA from the Fukushima Dai-ichi reactor accident. *J. Environ. Radioact.* **2012**, *112*, 165−170.
(38) Paatero, J.; Vira, J.; Siitari-Kauppi, M.; Hatakka, J.; Holmén, K.; Viisanen, Y. Airborne fission products in the high Arctic after the Fukushima nuclear accident. *J. Environ. Radioact.* **2012**, *114*, 41−47.
(39) Pentreath, R. J. *Nuclear power; man and the environment*; Taylor & Francis LTD: London, UK, 1980.
(40) Ten Hoeve, J. E.; Jacobson, M. Z. Worldwide health effects of the Fukushima Daiichi nuclear accident. *Energ. Environ. Sci.* **2012**, *5*, 8743−8757.
(41) *The "EPIC" impact assessment framework: Towards the protection of the Arctic environment from the effects of ionising radiation*; Brown, J. E., Thørring, H., Hosseini, A., Barnett, C. L., Børretzen, P., Beresford, N., Golikov, S., Kryshev, I., Oughton, D. H., Sazykina, T., Stensrud, H., Wright, S. M., Eds.; Deliverable D6 report for EU Funded Project ICA2-CT-2000-10032, Norwegian Radiation Protection Authority: Østerås, Norway, 2003; https://wiki.ceh.ac.uk/download/attachments/115802239/EPIC_D6.pdf?version=1&modificationDate=1263909651000.
(42) Larsson, C. -M The FASSET Framework for assessment of environmental impact of ionising radiation in European ecosystems e an overview. *J. Rad. Prot.* **2004**, *24*, A1−A12, DOI: 10.1088/0952-4746/24/4A/001.
(43) Larsson, C. M. An overview of the ERICA Integrated Approach to the assessment and management of environmental risks from ionising contaminants. *J. Environ. Radioact.* **2008**, *99*, 1364−1370.
(44) Kinoshita, N.; Sueki, K.; Sasa, K.; Kitagawa, J.; Ikarashi, S.; Nishimura, T.; Wong, Y. -S.; Satou, Y.; Handa, K.; Takahashi, T.; Sato, M.; Yamagata, T. Assessment of individual radionuclide distributions from the Fukushima nuclear accident covering central-east Japan. *P. Natl. Acad. Sci. USA* **2011**, *108* (49), 19526−19529.
(45) Bowyer, T. W.; Biegalski, S. R.; Cooper, M.; Eslinger, P. W.; Haas, D.; Hayes, J. C.; Miley, H. S.; Strom, D. J.; Woods, V. Elevated radioxenon detected remotely following the Fukushima nuclear accident. *J. Environ. Radioact.* **2011**, *102*, 681−687.
(46) Diaz Leon, J.; Jaffe, D. A.; Kaspar, J.; Knecht, A.; Miller, M. L.; Robertson, R. G. H.; Schubert, A. G. Arrival time and magnitude of airborne fission products from the Fukushima, Japan, reactor incident as measured in Seattle. WA, USA. *J. Environ. Radioact.* **2011**, *102*, 1032−1038.
(47) United States Environmental Protection Agency (US EPA) Press release−December 2011. http://www.epa.gov/japan2011/rert/radnet-sampling-data.html (January 10, 2012).
(48) Hernández-Ceballos, M. A.; Hong, G. H.; Lozano, R. L.; Kim, Y. I.; Lee, H. M.; Kim, S. H.; Yeh, S. -W.; Bolívar, J. P.; Baskaran, M. Tracking the complete revolution of surface westerlies over Northern Hemisphere using radionuclides emitted from Fukushima. *Sci. Total Environ.* **2012**, *438*, 80−85.
(49) Hong, G. H.; Hernández-Ceballos, M. A.; Lozano, R. L.; Kim, Y. I.; Lee, H. M.; Kim, S. H.; Yeh, S. W.; Bolívar, J. P.; Baskaran, M. Radioactive impact in South Korea from the damaged nuclear reactors in Fukushima: and evidence of the long and short transports. *J. Radiol. Prot.* **2012**, *32* (4), 397−411.
(50) Morino, Y.; Ohara, T.; Nishizawa, M. Atmospheric behavior, deposition, and budget of radioactive materials from the Fukushima Daiichi nuclear power plant in March 2011. *Geophys. Res. Lett.* **2011**, *38*, L00G11 DOI: 10.1029/2011GL048689.
(51) *Regulations for the safe transport of radioactive material*; IAEA Safety Requirements; International Atomic Energy Agency (IAEA): Vienna, Austria, 2005; no. TS-R-1; http://www-pub.iaea.org/mtcd/publications/pdf/pub1225_web.pdf.
(52) *Regulations for the safe transport of radioactive material*; IAEA Safety Requirements; International Atomic Energy Agency (IAEA): Vienna, Austria, 2009; no. TS-R-1; http://www-pub.iaea.org/MTCD/publications/PDF/Pub1384_web.pdf.
(53) Legarda, F.; Romero, L. M.; Herranz, M.; Barrera, M.; Idoeta, R.; Valiño, F.; Olondo, C.; Caro, A. Inventory and vertical migration of ^{137}Cs in Spanish mainland soils. *J. Environ. Radioact.* **2011**, *102*, 589−597.
(54) Shinonaga, T.; Schimmack, W.; Gerzabek, M. H. Vertical migration of ^{60}Co, ^{137}Cs and ^{226}Ra in agricultural soils as observed in lysimeters under crop rotation. *J. Environ. Radioact.* **2005**, *79*, 93−106.

(55) Golikov, V. Yu.; Balonov, M. I.; Jacob, P. External exposure of the population living in areas of Russia contaminated due to the Chernobyl accident. *Radiat. Environ. Bioph.* **2002**, *41* (10), 185−193.
(56) Hamada, N.; Ogino, H. Food safety regulations: what we learned from the Fukushima nuclear accident. *J. Environ. Radioact.* **2012**, *111*, 83−99.
(57) Harada, K. H.; Fujii, Y.; Adachi, A.; Tsukidate, A.; Asai, F.; Koizumi, A. Dietary intake of radiocesium in adult residents in Fukushima prefecture and neighboring regions after the Fukushima Nuclear Power Plant accident: 24 h-food duplicate survey in December 2011. *Environ. Sci. Technol.* **2012**, DOI: 10.1021/es304128t.
(58) *Exposures of the public and workers from various sources of radiation*; Report to the General Assembly with scientific annexes; United Nations Scientific Committee on the Effects of Atomic Radiation (UNSCEAR): United Nations, New York, 2008; Vol. *1* Annex B; http://www.unscear.org/docs/reports/2008/11-80076_Report_2008_Annex_D.pdf.
(59) *Medical radiation exposures*; Report to the General Assembly with scientific annexes; United Nations Scientific Committee on the Effects of Atomic Radiation (UNSCEAR): United Nations, New York, 2008; Vol. *1*, Annex A; http://www.unscear.org/docs/reports/2008/09-86753_Report_2008_Annex_A.pdf.
(60) De Cort, M.; Dubois, G.; Fridman, S. D.; Germenchuk, M. G.; Izrael, Y. A.; Janssens, A.; Jones, A. R.; Kelly, G. N.; Kvasnikova, E. V.; Matveenko, I. I.; Nazarov, I. M.; Pokumeiko, Y. M.; Sitak, V. A.; Stukin, E. D.; Tabachny, L. Y.; Tsaturov, Y. S.; Avdyushin, S. I. *Atlas of caesium deposition on Europe after the Chernobyl accident*; Office for Official Publications of the European Communities: Luxembourg, 1998; ISBN 92−828−3140-X, Catalogue number CG-NA-16-733-29-C. EUR 16733, pp 1−63.
(61) Møller, A. P.; Hagiwara, A.; Matsui, S.; Kasahara, S.; Kawatsu, K.; Nishiumi, I.; Suzuki, H.; Ueda, K.; Mousseau, T. A. Abundance of birds in Fukushima as judged from Chernobyl. *Environ. Pollut.* **2012**, *164*, 36−39.
(62) Hiyama, A.; Nohara, C.; Kinjo, S.; Taira, W.; Gima, S.; Tanahara, A.; Otaki, J. M. The biological impacts of the Fukushima nuclear accident on the pale grass blue butterfly. *Sci. Rep.* **2012**, *2*, 570 DOI: 10.1038/srep00570.
(63) Møller, A. P.; Nishiumi, I.; Suzuki, H.; Ueda, K.; Mousseau, T. A. Differences in effects of radiation on abundance of animals in Fukushima and Chernobyl. *Ecol. Indic.* **2013**, *24*, 75−81.
(64) Garnier-Laplace, J.; Beaugelin-Seiller, K.; Hinton, T. G. Fukushima wildlife dose reconstruction signals ecological consequences. *Environ. Sci. Technol.* **2011**, *45*, 5077−5078.
(65) Shozugawa, K.; Nogawa, N.; Matsuo, M. Deposition of fission and activation products after the Fukushima Dai-ichi nuclear power plant accident. *Environ. Pollut.* **2012**, *163*, 243−247.

■ NOTE ADDED AFTER ASAP PUBLICATION

There were errors in the units of the abstract graphic in the version of this paper published May 14, 2013. The correct version published May 16, 2013.